J Mater Sci (2009) 44:3751–3757
DOI 10.1007/s10853-009-3502-z

Effects of Nb_2O_5 doping on the microstructure and the dielectric temperature characteristics of barium titanate ceramics

Y. Yuan · S. R. Zhang · X. H. Zhou · B. Tang

Received: 25 October 2008 / Accepted: 17 April 2009 / Published online: 6 May 2009

Abstract In this work, the effects of Nb_2O_5 addition on the dielectric properties and phase formation of $BaTiO_3$ were investigated. A core–shell structure was formed for Nb-doped $BaTiO_3$ resulted from a low diffusivity of Nb^{5+} ions into $BaTiO_3$ when grain growth was inhibited. In the case of 0.3–4.8 mol% Nb_2O_5 additions, two dielectric constant peaks were observed. The Curie dielectric peak was determined by the ferroelectric-paraelectric transition of grain core, whereas the secondary broad peak at lower temperature was due to strong chemical inhomogeneity in Nb-doped $BaTiO_3$ ceramics. The dielectric constant peak at Curie temperature was markedly depressed with the addition of Nb_2O_5. On the other hand, the secondary dielectric constant peak was enhanced when sintered above 1280 °C for higher Nb_2O_5 concentrations ($\geq$1.2 mol%). The Curie temperature was shifted to higher temperatures, whereas the transition temperature corresponding to the secondary peak moved to lower temperatures as increasing the amount of Nb_2O_5 more than 1.2 mol%. The decrease of this lower transition temperature was assumed to be closely related with the secondary phase formation when Nb concentration greater than 1.2 mol%. From XRD analyses, a large amount of secondary phases was observed when Nb_2O_5 amount exceeded 1.2 mol%. The coefficients of thermal expansion of Nb-doped $BaTiO_3$ were increased with increasing Nb_2O_5 contents, resulting in large internal stress between cores and shells. Therefore, the shift of Curie temperature to higher temperatures was attributed to internal stress resulting from the formation of a core–shell structure and a large amount of secondary phase grains.

Introduction

Barium titanate ($BaTiO_3$, BT) is well known as one of the most widely studied and used perovskite ferroelectrics. It has a ferroelectric tetragonal structure at room temperature and changes to a paraelectric cubic structure on heating. The ferroelectric phase-transition temperature, called as Curie temperature or T_C, is a key factor for preparation of $BaTiO_3$-based temperature-stable capacitors because dielectric constant will decrease sharply above T_C according to the Curie–Weiss law $\varepsilon = C/(T - T_C)$ [1]. Hence, increasing the Curie temperature of $BaTiO_3$ is favorable in improving the temperature stability of dielectric constant so as to meet the requirement of high-temperature capacitors.

The Curie temperature is affected by such many factors as modification of chemical composition [2–5], particle and grain size [6, 7], tetragonality [7, 8], oxygen vacancies concentration [9, 10], stress [4, 5, 11, 12], and so on. The doping effects on the T_C of $BaTiO_3$ have been extensively investigated. As is well known, most impurity additions lower the Curie temperature of $BaTiO_3$. The Nb-doping effect on the Curie temperature of $BaTiO_3$ has been reported by many researchers. Kahn reported that the Curie temperature of $BaTiO_3$ was shifted to lower temperatures by Nb addition when significant grain growth happened. Contrarily, the Curie temperature of $BaTiO_3$ moved to higher temperatures for small-grained $BaTiO_3$ ceramics when grain growth was inhibited [13]. Cui et al. [14] reported that the Curie temperature of $BaTiO_3$ was

---

Y. Yuan (✉) · S. R. Zhang · X. H. Zhou · B. Tang
State Key Laboratory of Electronic Thin Film and Integrated Devices, University of Electronic Science and Technology of China, Chengdu 610054, People's Republic of China
e-mail: yingyuan@uestc.edu.cn

decreased by Nb addition. In view of these inconsistent results, the present study focused on the investigation of the effect of Nb addition on the dielectric properties of $BaTiO_3$. The results proved that Nb shifted the Curie temperature to higher temperatures. This paper discusses the influence of Nb-doping on the Curie temperature of $BaTiO_3$ and possible mechanism.

Experimental procedure

Samples were prepared from commercial $BaTiO_3$ powder (GuoTeng Ceramic Inc., average grain size 0.4 µm, Ba/Ti = 1) doped with 0.3, 0.6, 1.2, 2.4, 3.6, or 4.8 mol% Nb_2O_5 (99% purity) by the conventional ceramic processing technique. Then, 1 mol% $BaSiO_3$ was used as sintering aid. Raw materials were ball-milled in deionized water for 8 h. The prepared ceramic powders were pressed in disk form (10 mm in diameter and 1 mm thick) by mixing ceramic powders with 3 wt% PVA binder. After debindering, the disks were finally fired at 1240–1320 °C for 2 h in air. Fired-on-silver was used as electrodes for the measurement of electric properties. Dielectric measurement of samples was performed by using a LCR meter (YY2812) auto-controlled by computer at 1 kHz and 1.0 V rms in the temperature range from −55 to 200 °C. Microstructures of the ceramics were observed using an S-530 scanning electron microscope (SEM). The X-ray diffraction (XRD) analysis was carried out using a Philips X'Pert diffract meter over the range of $2\theta = 20\text{–}60°$ with Cu$\kappa\alpha$ radiation.

The recently developed software Material Analysis Used Diffraction (MAUD), which is based on a Rietveld method combined with a Fourier analysis, has been applied to analyze the XRD of alloys and ferroelectrics [4, 15–17]. In our work, the structural refinement was carried out by using MAUD. The coefficients of thermal expansion for pure $BaTiO_3$ and Nb-doped $BaTiO_3$ ceramics were measured by thermal expansion meter with a heating rate of 5 °C/min. The coefficient of thermal expansion was calculated by Eq. 1:

$$\bar{\alpha} = \frac{1}{L_0} \cdot \frac{L_2 - L_1}{T_2 - T_1} + \alpha_0 \tag{1}$$

where L_0 is the length of sample at room temperature, L_1, L_2 is the length of sample at T_1 and T_2, respectively, and α_0 is the coefficient of thermal expansion of quartz (5.7×10^{-7}/°C).

Results and discussion

SEM micrographs for samples sintered at 1280 °C with various Nb_2O_5 contents were shown in Fig. 1. When 0.3–2.4 mol% Nb_2O_5 was added, the microstructure was homogeneous fine grained and rather porous (Fig. 1a–d). As Nb_2O_5 concentration increased further (≥3.6 mol%), significant grain growth occurred and the proportion of pores decreased (Fig. 1e, f). As Nb_2O_5 content increased to 1.2 mol%, secondary phase began to occur which was proved by XRD analysis. However, it was hard to observe the secondary phase grains by SEM due to the formation of small amount of secondary phase. Figure 2 shows the grain morphology of samples sintered at 1320 °C doped with 0.3, 1.2 and 2.4 mol% Nb_2O_5, respectively. It was observed that sintering temperature had little effect on the size of matrix grains for Nb-doped $BaTiO_3$ ceramics. As 0.3–1.2 mol% Nb_2O_5 was doped, no secondary phase appeared (Fig. 2a, b). With 2.4 mol% Nb_2O_5 addition, two types of grains were observed, that is, the matrix composed of fine grains and large secondary phase grains (Fig. 2c).

The phase formation of samples sintered at 1280 °C with different Nb_2O_5 contents (0.6–4.8 mol%), as examined by XRD is shown in Fig. 3. It was obvious that the perovskite $BaTiO_3$ phase was formed in all samples. With an addition of 0.6 mol% Nb_2O_5, no additional peak representing a secondary phase was observed. However, secondary phases were detected when Nb_2O_5 amount exceeded 1.2 mol%. The composition of the secondary phases was identified as $Ba_6Ti_{14}Nb_2O_{39}$, $Ba_3Ti_5Nb_{3.2}O_{21}$, and $Ba_6Ti_{17}O_{40}$. Therefore, it was assumed that the solubility limit of Nb_2O_5 in $BaTiO_3$ at 1280 °C in air was less than 1.2 mol%. The secondary phase formation was due to the substitution of Nb^{5+} to Ti^{4+} site and segregation of Ti^{4+} out of $BaTiO_3$ grains [18].

Figure 4a shows the temperature dependence of dielectric constant for $BaTiO_3$ ceramics sintered at 1240 °C with various Nb_2O_5 contents. With 0.3 mol% Nb_2O_5 addition, two dielectric constant peaks were observed. A core–shell structure was developed for small grained $BaTiO_3$ ceramics during sintering because of low diffusivity of Nb^{5+} ions into $BaTiO_3$ lattice [19]. The core was composed of pure barium titanate, while the shell was doped with additive Nb. The maximum of dielectric constant at 133 °C was determined by the phase transition from ferroelectric to paraelectric of unreacted pure $BaTiO_3$ grain core so that this temperature was called Curie temperature or T_C. On the other hand, the dielectric constant peak at a lower temperature of 45 °C was broad and diffuse due to strong chemical inhomogeneity in Nb-doped $BaTiO_3$ ceramics. The transition temperature corresponding to the secondary broad peak was denoted as T_1. With an increase of Nb_2O_5 content, the dielectric constant peak at T_C was obviously depressed, especially in the cases of ≥1.2 mol% Nb_2O_5 additions. It is also shown in Fig. 4a that T_1 shifts to lower temperatures as Nb amount exceeded 1.2 mol%. With >3.6 mol% Nb_2O_5 addition, the secondary dielectric constant peak even could not be

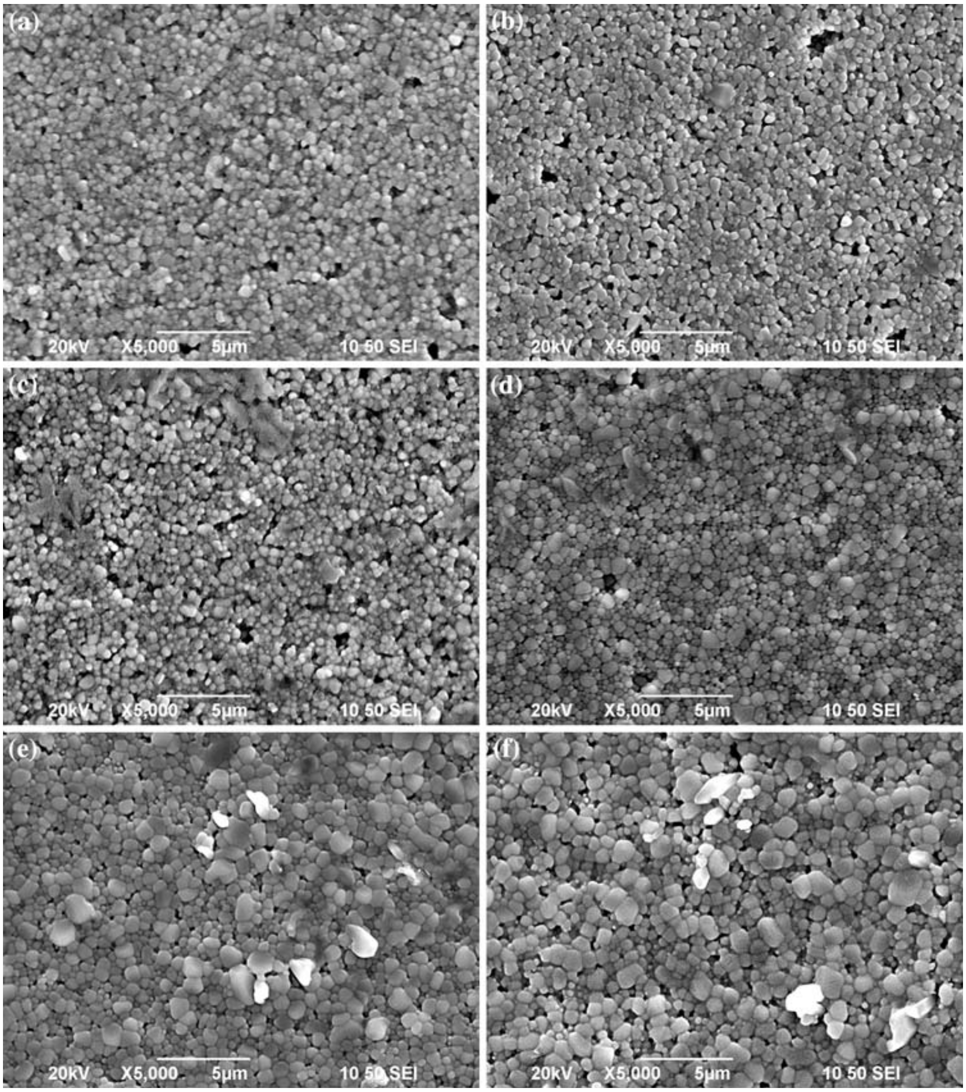

Fig. 1 SEM micrographs of Nb_2O_5-doped $BaTiO_3$ ceramics sintered at 1280 °C. Nb_2O_5 contents of these samples were **a** 0.3, **b** 0.6, **c** 1.2, **d** 2.4, **e** 3.6, and **f** 4.8 mol%

observed in the temperature range of −55 to 200 °C. This indicated that Nb made T_1 lower than −55 °C for higher Nb_2O_5 concentrations (>3.6 mol%). Figure 4b and c shows the temperature dependence of dielectric constant for Nb-doped $BaTiO_3$ ceramics sintered at 1280 and 1320 °C with various Nb_2O_5 contents, respectively. It is obvious that the curves in Fig. 4b and c are similar to those in Fig. 4a. The impact of sintering temperature on the temperature dependence of dielectric constant is slight for the sample doped with 0.3 mol% Nb_2O_5, which suggested that the grain shell is thin when a low concentration Nb_2O_5 was added. However, as Nb_2O_5 concentration exceeded 1.2 mol%, the dielectric constant peak at T_C was greatly depressed, whereas the dielectric constant peak at lower temperature was enhanced with increasing sintering temperature. Especially, for the samples doped with more than 3.6 mol% Nb_2O_5, the Curie peak disappeared by sintering at temperature above 1280 °C, indicating the collapse of core–shell structure and homogeneous distribution of Nb in $BaTiO_3$. High sintering temperature promoted solid-state diffusion and caused the core–shell structure to disappear.

Figure 5 shows the dependences of T_C and T_1 on Nb_2O_5 contents for Nb-doped $BaTiO_3$ ceramics sintered at 1240, 1280, or 1320 °C, respectively. With increasing the amount of Nb_2O_5, T_C increased, while T_1 was independent of Nb content up to 1.2 mol% and then decreased rapidly with further addition. It was observed that T_1 was almost unchanged for lower Nb_2O_5 concentrations (≤1.2 mol%). Moreover, sintering temperature has no effect on T_1 at Nb_2O_5 content less than 1.2 mol%. It has been known that high sintering temperature promoted solid-state diffusion of Nb and caused the volume fraction of grain shell to increase. Therefore, it was assumed that T_1 had little to do with the volume fraction of grain shell. For higher Nb_2O_5 concentrations (>1.2 mol%), T_1 was related with Nb content, that is, T_1 was almost decreased linearly as Nb_2O_5 increased. Moreover, T_1 shifted to lower temperatures by increasing sintering temperature from 1240 to 1280 °C. It

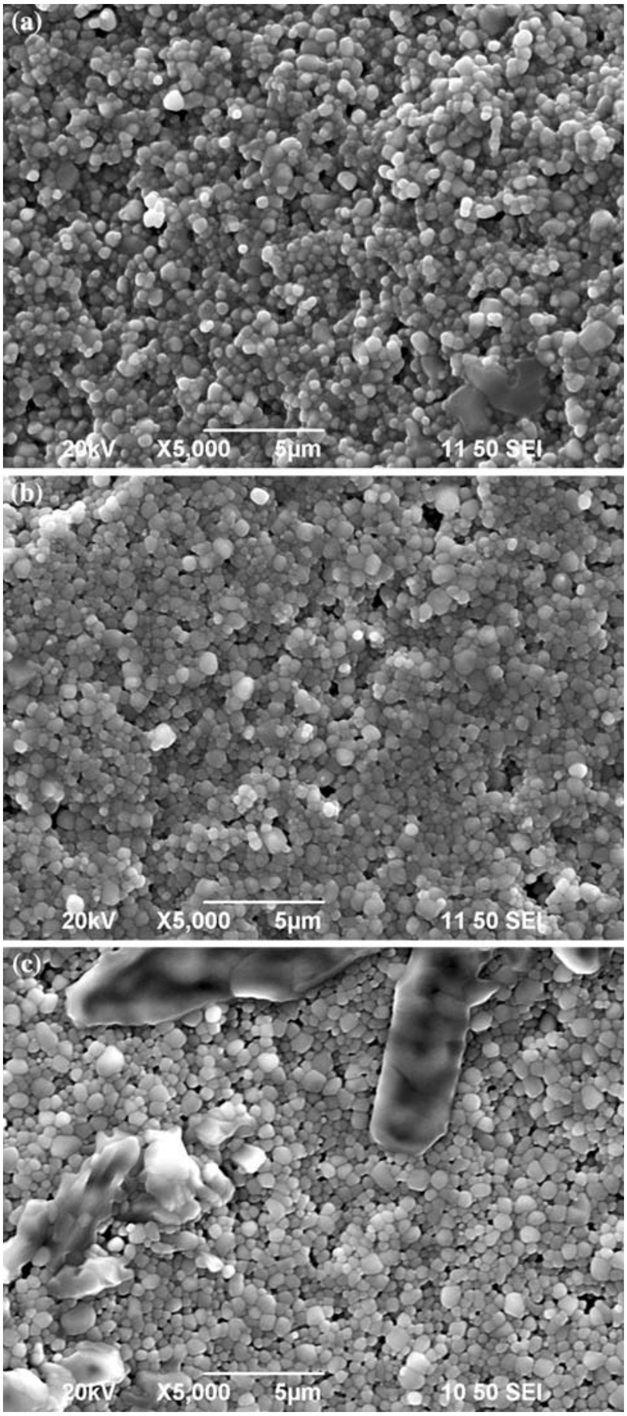

Fig. 2 SEM micrographs of Nb_2O_5-doped $BaTiO_3$ ceramics sintered at 1320 °C. Nb_2O_5 contents of these samples were **a** 0.3, **b** 1.2, and **c** 2.4 mol%

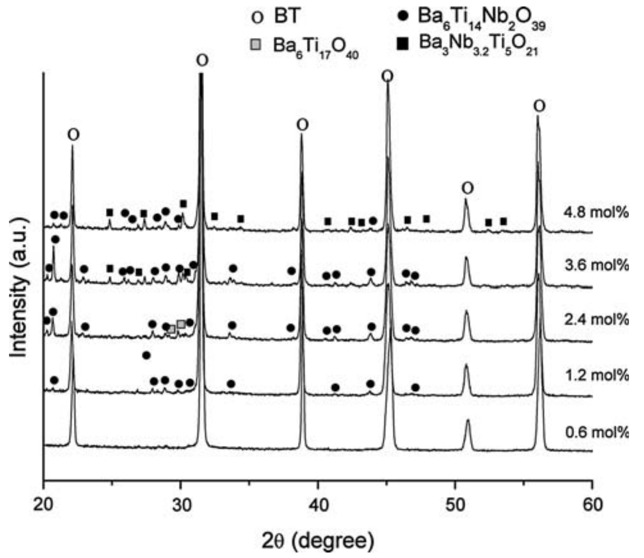

Fig. 3 X-ray diffactograms of samples with various Nb_2O_5 contents

was analyzed by XRD that the solubility limit of Nb_2O_5 in $BaTiO_3$ was less than 1.2 mol%. At Nb_2O_5 content above 1.2 mol%, secondary phase appeared and the amount of the secondary phase increased with an increase in Nb_2O_5 content and sintering temperature. Therefore, the decrease of T_1 was assumed to be correlated with the secondary phase formation when Nb_2O_5 concentration is greater than 1.2 mol%.

In contrast to T_1, T_C shifted to higher temperatures with Nb_2O_5 addition in the present study. According to ionic size, Nb^{5+} ions preferentially substituted to Ti^{4+} and extra positive charge could be compensated by V''_{Ba} and/or V''''_{Ti}. It was well accepted that the coupling of TiO_6 oxygen octahedral played a critical role in the stability of ferroelectric phase in $BaTiO_3$ perovskite [20]. The degree of the coupling between neighboring TiO_6 octahedra or the stability of ferroelectric phase would be significantly weakened by introducing defects. Therefore, Nb addition would shift the Curie temperature of $BaTiO_3$ to lower temperatures. Kahn [13] reported that incorporation of single Nb decreased the Curie temperature in large-grained $BaTiO_3$ and small-grained $BaTiO_3$ grown from ultrafine powder, in agreement also with results by Hennings and Rosenstein [3] and Cui et al. [14]. During sintering, Nb^{5+} ions diffused into $BaTiO_3$ lattice and a core–shell structure would be formed due to a low diffusivity of Nb^{5+}. However, the diffusion of Nb^{5+} ions was enhanced and the core–shell structure would be destroyed as significant grain growth happened, which led to a homogeneous distribution of Nb in $BaTiO_3$ [13, 21]. We attributed the decrease of T_C in their work to a homogeneous distribution of Nb in $BaTiO_3$. In our study, a core–shell structure was formed, which was proved by the double dielectric constant peak in Fig. 4. The shift of Curie temperature to higher temperatures resulted from the internal stress existing in core–shell structure grains. As discussed earlier, T_C was correlated with the ferroelectric-paraelectric phase transition of grain core. Jung et al. [5], Song et al. [12], and Hwang et al. [22] have suggested that

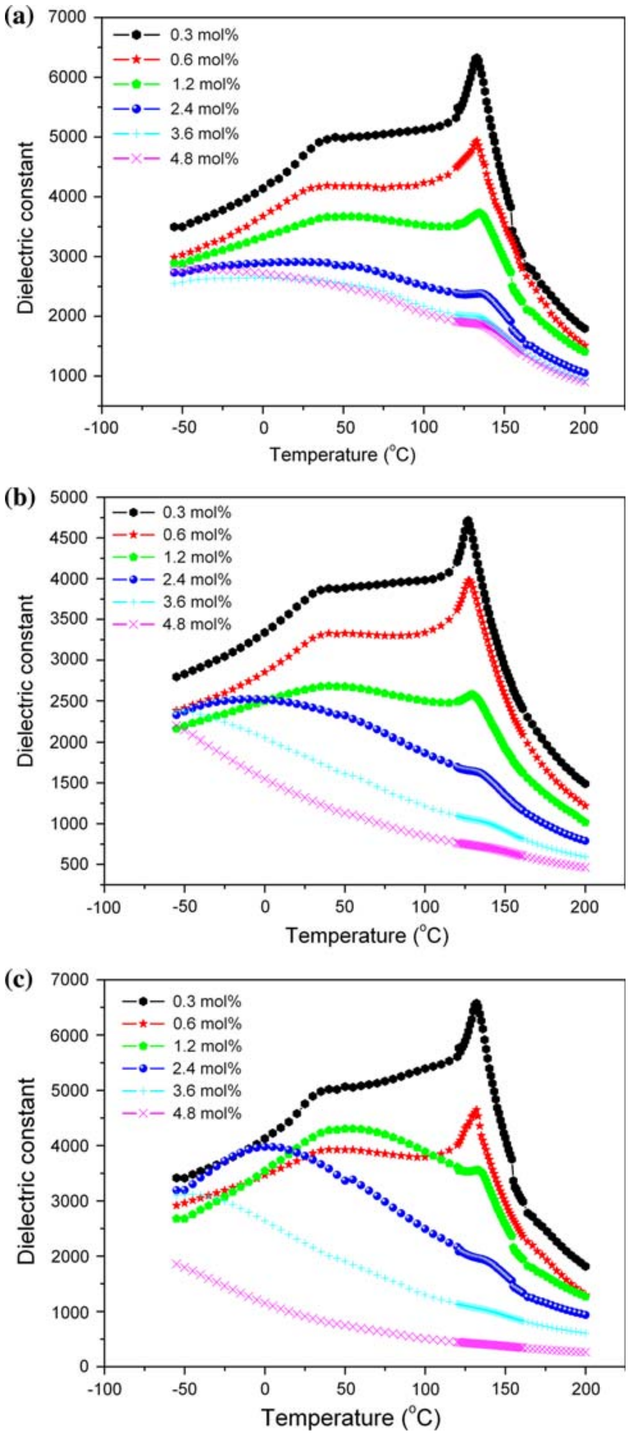

Fig. 4 Temperature dependence of dielectric constant for $BaTiO_3$ ceramics with various Nb_2O_5 contents: **a** 1240 °C, **b** 1280 °C, and **c** 1320 °C

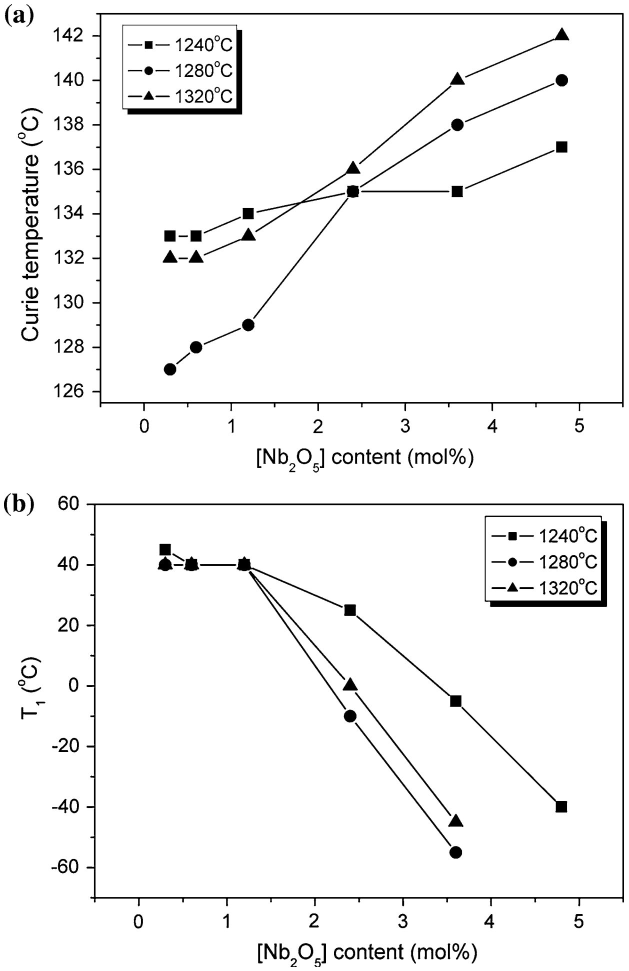

Fig. 5 Curie temperature T_C and T_1 as functions of Nb_2O_5 contents for $BaTiO_3$ ceramics sintered at 1240, 1280, and 1320 °C, respectively

the addition of smaller ionic radius rare earth elements moved T_C to higher temperatures in samples composed of a core–shell structure in the $BaTiO_3$–MgO–Re_2O_3 (Re = Ho, Er, Yb, Lu, Y) system. The dielectric constant peak at T_C was substantially determined by the cubic-tetragonal phase transition of unreacted pure $BaTiO_3$ grain core. They attributed the shift of T_C to the internal stress existing in core–shell structure grains resulting from the thermal expansion mismatch between cores and shells. It is well accepted that the ferroelectric phase transition of $BaTiO_3$ is affected by stress, including external stress [1, 23] and internal stress [5, 11, 12, 22]. Curie temperature was shifted to lower temperatures by compaction external stress. Recently, the effect of internal stress on the Curie temperature of $BaTiO_3$ has been investigated. It was found by microindentation analysis that internal stress remaining in core–shell structure grains was much higher than that in chemical homogeneous grains, leading to a significant shift of Curie temperature [24]. Internal stress arose from the thermal expansion mismatch between grain cores and grain shells. Therefore, we examined the thermal expansion curves of pure $BaTiO_3$ and Nb-doped $BaTiO_3$ ceramics sintered at 1280 °C with various Nb_2O_5 contents, as shown in Fig. 6. The thermal expansion coefficients calculated

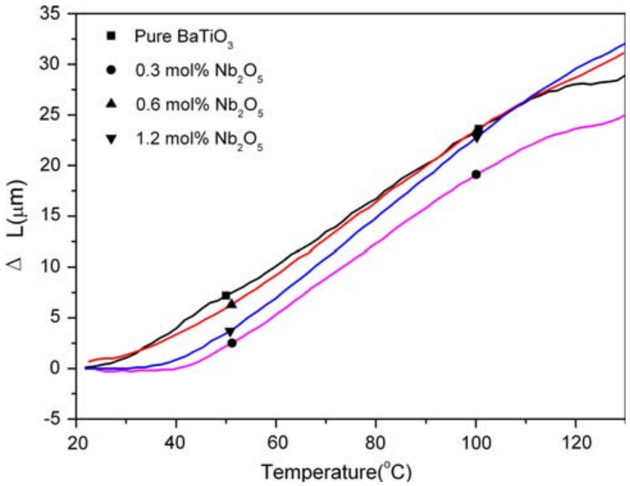

Fig. 6 Thermal expansion curves of pure $BaTiO_3$ and Nb_2O_5-doped $BaTiO_3$ ceramics sintered at 1280 °C with various Nb_2O_5 contents

Table 1 Thermal expansion coefficient of pure $BaTiO_3$ and Nb_2O_5-doped $BaTiO_3$ ceramics sintered at 1280 °C

Nb_2O_5 (mol%)	T_0 (°C)	ΔL_0 (μm)	T (°C)	ΔL_t (μm)	L_0 (mm)	α_L (ppm/°C)
0	50.0	7.2	99.0	23.0	51.98	6.772
0.3	51.2	2.5	100.1	19.1	53.58	6.906
0.6	51.1	6.3	100.2	23.4	54.18	6.998
1.2	50.8	3.7	100.2	22.8	53.44	7.805

from Fig. 6 are given in Table 1. It could be concluded that the thermal expansion coefficients of Nb-doped $BaTiO_3$ ceramics increased with an increase in Nb_2O_5 contents. The ferroelectric core is pure barium titanate and the paraelectric shell was doped with additive Nb_2O_5. It was suggested that core and shell regions could not be totally separated in core–shell structure grains [3]. Therefore, it was reasonable to deduce that the thermal expansion coefficient of core–shell structure grains was a summation of those of cores and shells. Moreover, it was indicated from our results that the thermal expansion coefficient of shells was larger than that of pure barium titanate cores. According to high expansion of grain shell, pure barium titanate cores were exposed to compaction stress as cooling to room temperature. Moreover, the compaction stress placed on cores increased with increasing Nb_2O_5 contents, due to an increase of the thermal expansion coefficient of grain shells.

On the other hand, according to Buessem et al. [25, 26], every grain in fine grained ceramics was subjected to a complex internal stress that depended on the orientation of all surrounding grains. From XRD analyses, a large amount of secondary phase grains existed with Nb_2O_5 content greater than 1.2 mol%. Thus, it was considered that Nb-doped $BaTiO_3$ grains were subjected to large internal stress resulting from the formation of a core–shell structure and secondary phase grains. In order to determine the microstrain of samples sintered at 1280 °C, the XRD patterns were subjected to detailed microstructure study by using MAUD. The results are reported in Fig. 7. The Curie temperature as a function of Nb_2O_5 contents is also shown in Fig. 7. It could be seen that microstrain increased continuously with an increase in Nb_2O_5 amount, and Curie temperature showed the same trend as microstrain. The Curie temperature moved from 127 to 140 °C in the case of 4.8 mol% Nb_2O_5 addition. This was an indication that the Curie temperature of $BaTiO_3$ ceramics was dependent on microstrain to a certain extent.

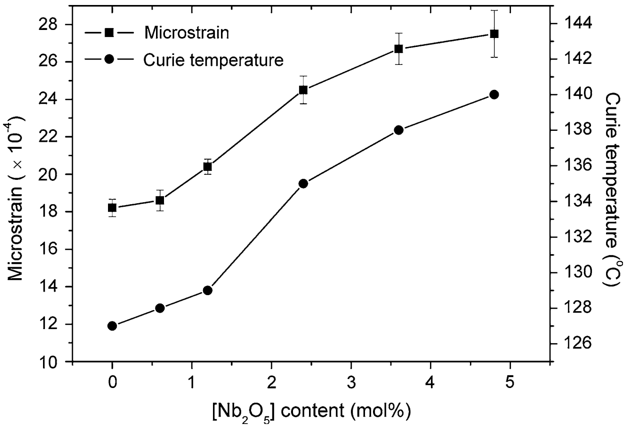

Fig. 7 Microstrain and Curie temperature as functions of Nb_2O_5 contents for $BaTiO_3$ ceramics sintered at 1280 °C

Conclusion

Homogeneous and fine grained microstructure was observed in Nb_2O_5-doped $BaTiO_3$ ceramics sintered at 1280 °C. For higher Nb_2O_5 concentration (≥2.4 mol%), large secondary phase grains occurred when sintered at 1320 °C. XRD analysis proved that secondary phase was detected when the Nb_2O_5 amount exceeded 1.2 mol%, which was identified as $Ba_6Ti_{14}Nb_2O_{39}$, $Ba_3Ti_5Nb_{3.2}O_{21}$, and $Ba_6Ti_{17}O_{40}$. It was found Nb_2O_5 addition played an important role in the transition temperature of $BaTiO_3$ ceramics. As the amount of Nb_2O_5 was increased, T_C was shifted to higher temperatures. Contrarily, T_1 was independent of Nb_2O_5 content up to 1.2 mol% and then decreased rapidly with further addition. The decrease of T_1 was assumed to be correlated with the secondary phase formation when Nb_2O_5 concentration was greater than 1.2 mol%. On the other hand, the shift of T_C to higher temperatures was attributed to large internal stress in Nb_2O_5-doped $BaTiO_3$ ceramics. The internal stress originates not only from the misfit between grain cores and grain shells in core–shell structure, but also from the formation of the large secondary phase grains.

References

1. Merz WJ (1953) Phys Rev 91:513
2. Lin JN, Wu TB (1990) J Appl Phys 68:985
3. Hennings D, Rosenstein G (1984) J Am Ceram Soc 67:249
4. Tang B, Zhang SR, Yuan Y. J Mater Sci Mater Electron. doi: 10.1007/s10854-007-9477-0
5. Jung YS, Na ES, Paik U (2002) Mater Res Bull 37:1633
6. Arlt G, Hennings D, de With G (1985) J Appl Phys 58:1619
7. Uchino K, Sadanaga E, Hirose T (1989) J Am Ceram Soc 72:1555
8. Begg BD, Vance ER, Nowotny J (1994) J Am Ceram Soc 77:3186
9. Albertsen K, Hennings D, Steigelmann O (1998) J Electroceram 2(3):193
10. Lee S et al (2007) J Appl Phys 101:054119
11. Sato S, Fujikawa Y, Nomura T (2000) Am Ceram Soc Bull 79:155
12. Song YH, Hwang JH, Han YH (2005) Jpn J Appl Phys 44:1310
13. Kahn M (1971) J Am Ceram Soc 54:455
14. Cui B, Yu PF, Tian J (2007) Mater Sci Eng A 454–455:667
15. Sahu P, Pradhan SK, De M (2004) J Alloys Compd 377:103
16. Cont L et al (2002) Ferroelectrics 267:323
17. Iverson BJ, Jones JL, Bowman KJ (2006) Phys B Condens Matter 385–386:581
18. Brzozowski E, Castro MS, Foschini CR (2002) Ceram Int 28:773
19. Chiang SK, Lee WE, Readey DW (1987) Am Ceram Soc Bull 66:1230
20. Thomas NW (1990) J Phys Chem Solids 51:1419
21. Chazono H, Kishi H (2000) J Am Ceram Soc 83:101
22. Hwang JH, Choi SK, Han YH (2001) Jpn J Appl Phys 40:4952
23. Samara GA (1966) Phys Rev 151:378
24. Armstrong TR, Buchanan RC (1990) J Am Ceram Soc 73:1268
25. Buessem WR, Cross LE, Goswami AK (1966) J Am Ceram Soc 49:33
26. Buessem WR, Cross LE, Goswami AK (1966) J Am Ceram Soc 49:36